Talanta 93 (2012) 364–370

Contents lists available at SciVerse ScienceDirect

Talanta

journal homepage: www.elsevier.com/locate/talanta

Gold–silver-nanoclusters having cholic acid imprinted nanoshell

Aytaç Gültekin [a], Arzu Ersöz [b], Adil Denizli [c], Rıdvan Say [b,*]

[a] Department of Energy Systems Engineering, Karamanoğlu Mehmetbey University, Karaman, Turkey
[b] Department of Chemistry, Anadolu University, Eskişehir, Turkey
[c] Department of Chemistry, Hacettepe University, Ankara, Turkey

ARTICLE INFO

Article history:
Received 26 August 2011
Received in revised form 16 February 2012
Accepted 23 February 2012
Available online 3 March 2012

Keywords:
Gold–silver-nanoclusters
Molecularly imprinted polymers
Cholic acid
Photoluminesence

ABSTRACT

Molecular imprinted polymers (MIPs) as a recognition element for sensors are increasingly of interest and MIP-nanoparticles have started to appear in the literature. In this study, we have proposed a novel thiol ligand-capping method with polymerizable methacryloylamido-cysteine (MAC) attached to gold–silver-nanoclusters reminiscent of a self-assembled monolayer and have reconstructed surface shell by synthetic host polymers based on molecular imprinting method for cholic acid recognition. In this method, methacryloylamidohistidine–Pt(II) [MAH–Pt(II)] has used as a new metal-chelating monomer via metal coordination–chelation interactions and cholic acid. Nanoshell sensors with templates give a cavity that is selective for cholic acid. The cholic acid can simultaneously chelate to Pt(II) metal ion and fit into the shape-selective cavity. Thus, the interaction between Pt(II) ion and free coordination spheres has an effect on the binding ability of the gold–silver-nanoclusters nanosensor. The binding affinity of the cholic acid imprinted nanoparticles have investigated by using the Langmuir and Scatchard methods and determined affinity constant ($K_{affinity}$) has found to be 2.73×10^4 mol L^{-1} and 2.13×10^8 mol L^{-1}, respectively. At the last step of this procedure, cholic acid level in blood serum and urine which belong to a healthy people were determined by the prepared gold–silver-nanoclusters.

© 2012 Elsevier B.V. All rights reserved.

1. Introduction

Bile acids are important steroidal compounds which are synthesized from cholesterol in the liver, stored in the gall bladder, and released in the small intestine for the digestion of fats and lipids. The concentration of bile acids in body is related with hepatitis, gallstone and other diseases in liver. The qualitative and quantitative analysis of bile acids have both clinical and pharmaceutical significance. Medically, it is feasible to reduce cholesterol content in body by removing bile acids, especially for the treatment of hyperlipidemia [1,2]. It is thus important to prepare bile acid sorbents with high selectivity for analysis and potential medical applications [3]. Cholic acid as well as its derivatives is the main component of bile acids. Several methods such as liquid chromatography (LC) with UV detection [4–6], LC coupled to evaporative light scattering detection (ELSD) [7,8], ultra high-performance liquid chromatography–mass spectrometry (UHPLC) [9], have been applied for bile acids detection in serum but they use large and costly instruments and require sophisticated, frequently wide analysis procedures.

Molecular imprinting is a technology to create recognition sites in a macromolecular matrix using a molecular template [10]. In other words, both the shape image of the target and alignment of the functional moieties to interact with those in the target, are memorized in the macromolecular matrix for the recognition or separation of the target during formation of the polymeric materials themselves [11]. Molecularly imprinted polymers (MIPs) are easy to prepare, stable, inexpensive and capable of molecular recognition [12]. Therefore, MIPs can be considered as artificial affinity media. Molecular recognition-based separation techniques have received much attention in various fields because of their high selectivity for target molecules. Three steps are involved in the ion-imprinting process: (i) complexation of template (i.e., metal ions) to a polymerizable ligand, (ii) polymerization of this complex and (iii) removal of template after polymerization [13].

A nanoparticle which historically has included nanopowder, nanocluster, and nanocrystal is a small particle with at least one dimension less than 100 nm. A nanocluster is an amorphous/semicrystalline nanostructure. This distinction is an extension of the term "cluster" which is used in inorganic/organometallic chemistry to indicate small molecular cages of fixed sizes [14]. In last decades, great research efforts have focused on nanoparticles with a prospect to their potential applications in nanoelectronics, sensor technology, non-linear optics, catalysts, hydrogen storage and solar technology [15]. Because of their large surface-to-volume ratio, quantum mechanic size effects

* Corresponding author at: Fen Fakültesi, Yunus Emre Kampüsü, Anadolu Universitesi, 26470 Eskişehir, Turkey. Tel.: +90 222 335 0580; fax: +90 320 4910.
E-mail address: rsay@anadolu.edu.tr (R. Say).

0039-9140/$ – see front matter © 2012 Elsevier B.V. All rights reserved.
doi:10.1016/j.talanta.2012.02.057

and curvature-induced surface effects nanoparticles exhibit novel properties, for example lower melting point, higher self-diffusion coefficient, lower effective Debye temperature, higher solid–solid phase transition pressure, decreased ferroelectric phase transition temperature, as well as changed thermophysical properties and size-dependent catalytic activity [16,17]. The interest in studying great with metallic and bimetallic nanoparticles because of both the fundamental understanding and potential technological applications. At a fundamental level, information on the evolution of electronic structures of small metallic particles and their effects on the optical absorption spectra continue to be a major goal of research on metal clusters and nanoparticles. On a practical level, the unusual optical properties of metallic nanoparticles are exploited for a variety of applications including optical markers for biomolecules, biological sensors, optical filters, surface enhancement in Raman spectroscopy and ultrafast non-linear optical devices [18–20].

In last years, the combination of nanoparticles and MIPs have been applied in selective sensing detection. The molecular imprinting nanotechnologies are expected to greatly enhance the molecular affinity of MIP materials, and thus provide a wider range of applications approaching to biological receptors. Nanostructured, imprinted materials have a small dimension with extremely high surface-to-volume ratio, so that most of template molecules are situated at the surface and in the proximity of materials surface. In the case of nanosized particles, most of imprinted sites are situated at the surface or in the proximity of surface. Therefore, the forms of imprinted materials are expected to greatly improve the binding capacity and kinetics and site accessibility of imprinted materials. The MIP nanospheres with 100-nm size had a higher binding capacity, which was 2.5 fold that of normal bulky particles with 5-μm size. On the other hand, the low-dimensional nanostructures with imprinted sites have very regular shapes and sizes, and the tunable flexibility of shapes and sizes. The imprinted nanomaterials have also better dispersibility in analyte solutions and thus greatly reduce the resistance of mass transfer, exhibiting a fast binding kinetics. The imprinted nanomaterials with well-defined morphologies can feasibly been installed onto the surface of devices in a required form for many applications in nanosensors and molecular detection [21]. Only a few application of nanoclusters/MIPs have been reported [22–24]. In this study, we have proposed a novel thiol ligand-exchange method using polymerizable methacryloylamidocysteine (MAC) of gold–silver-nanoclusters to cap by organic layer, reminiscent of a self-assembled monolayer and have reconstructed surface shell by synthetic host polymers based on molecular imprinting method for cholic acid recognition. Methacryloylamidohistidine–Pt(II) [MAH–Pt(II)], was used as a new metal-chelating monomer via metal coordination–chelation interactions and cholic acid. We have combined nanoscale materials with MIP considering the ability of cholic acid to chelate of Pt(II) ion of MAH monomer to create reminiscent ligand exchange (LE) assembled binding sites, because the Pt(II) primarily interacts with the cholic acid [25]. In this study, synthesis, characterization and efficiency of the gold–silver-nanoclusters sensor based on cholic acid imprinted polymer have investigated. Cholic acid level in blood serum and urine has determined using this Au–Ag nanosensor.

2. Experimental

2.1. General methods

Methacryloyl chloride, was supplied by Aldrich and used as received. Cholic acid and chenodeoxycholic acid were supplied by Sigma Aldrich and ethylene glycol dimethacrylate (EDMA) was obtained from Fluka A.G., distilled under reduced pressure in the presence of hydroquinone inhibitor and stored at 4 °C until use.

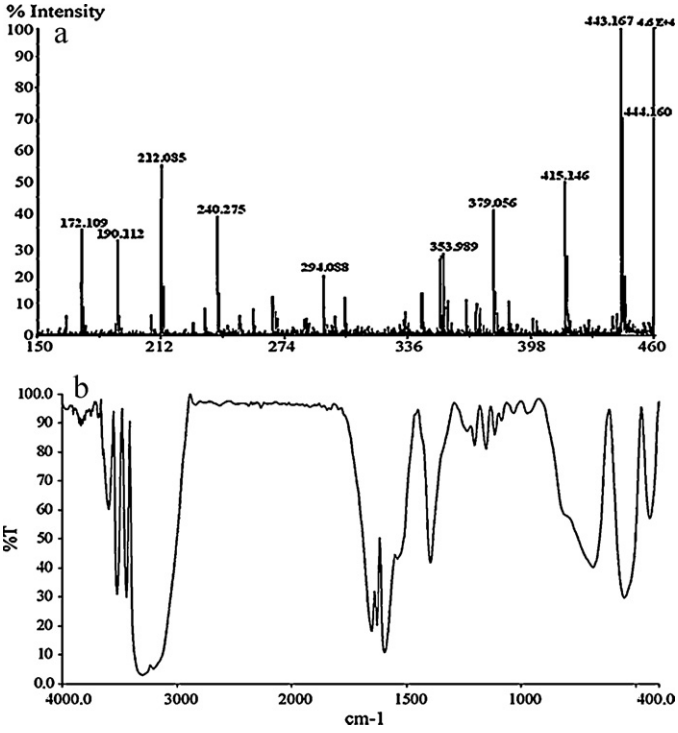

Fig. 1. (a) MALDI-TOF/MS spectrum of MAH-Pt(II) (2 μL of MAH-Pt(II) solution was mixed with 18 μL of a 10 mg mL^{-1} solution of CHCA in acetonitril/0.1% TFA. The acceleration voltage was set to 20 kV and the delay time was 100 ns and (b) FTIR spectrum of MAH-Pt(II).

Azobisisobutyronitrile (AIBN) was also supplied from Fluka. All other chemicals were of reagent grade and were purchased from Merck AG. All water used in the experiments was purified using a Barnstead NANOpure ultrapure water system.

Photoluminescence spectra were acquired by spectrofluorometer (Varian Cary Eclipse, Australia). ^{1}H and ^{13}C NMR spectra were recorded in DMSO-d_6 with TMS as the internal standard using Bruker 500 MHz NMR equipment. The Transmission Emission Microscopy (TEM) images of nanocrystals were acquired on a FEI-Tecnai^{TM} G^2 Sprit transmission electron microscope (20–120 kV). Sample preparation was consisted of drop coating the nanoclusters onto carbon-coated copper grids and air dried. Raman spectra images were obtained using a Raman Spectrophotometer (Bruker Senterra Dispersive Raman Microscope, Germany). Fourier Transform Infrared (FTIR) spectra images were obtained using a FTIR (Spectrum 100, Perkin Elmer, USA). For this purpose the dry beads (about 0.1 g) were thoroughly mixed with KBr (0.1 g, IR Grade, Merck, Germany), pressed into a pellet and then the FTIR spectrum was recorded.

2.2. Preparation of functional and metal-chelate monomers

MAC, monomer, was used for forming of reminiscent of self-assembled monolayer on the surface of nanoparticles and was synthesized and characterized according to the previously published procedure [26]. Histidine-functional monomer, MAH, was synthesized according to the previously published procedure [27] and characterized with ^{1}H NMR.

Data for MAH: ^{1}H NMR ($CDCl_3$): 1.99 (t; 3H, J = 7.08 Hz, CH_3), 1.42 (m; 2H, CH_2), 3.56 (t; 3H, $-OCH_3$), 4.82–4.87 (m; 1H, metil), 5.26 (s; 1H, vinil H), 5.58 (s; 1H, vinil), 6.86 (d; 1H, J = 7.4 Hz, NH), 7.82 (d; 1H, J = 8.4 Hz, NH), 6.86–7.52 (m; 5H, aromatic).

On the other hand, metal-chelate monomer, MAH–Pt(II), was synthesized according to the our previously published

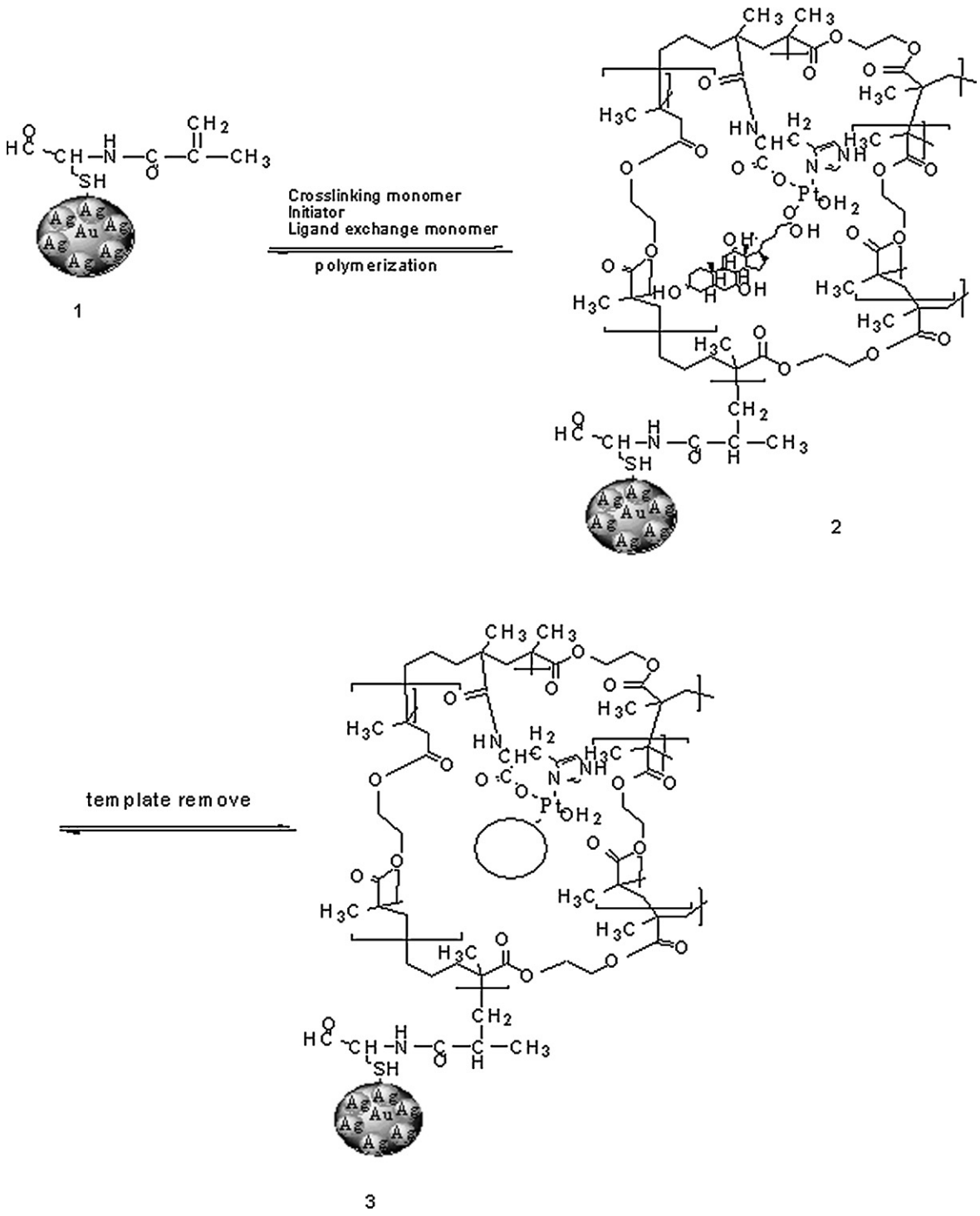

Fig. 2. Schematic illustration of cholic acid molecular imprinting on MAC modified Au–Ag nanoclusters (**1**). Au–Ag nanoclusters polymerized with AIBN, EDMA MAH–Pt(II)–cholic acid (**2**). Cholic acid removed with 12 mL (3/1, v/v) of 2 M NaOH/THF (**3**).

procedure [28]. MAH–Pt(II) was preorganized using MAH and $PtCl_2$. MAH (0.1 mmol) and $PtCl_2$. (0.1 mmol) were dissolved in 5.0 mL of aceton–water and the solution was stirred for 6 h. MAH–Pt(II) metal-chelate monomer was characterized with MALDI-TOF/MS (Fig. 1a). The ion peaks at 415 and 443 *m*/*z* confirms that MAH–Pt–$(H_2O)_2$ metal-chelate monomer structure was produced exactly. This situtation can be explained in the following way: if Pt is in 198 isotope form in MAH–Pt–$(H_2O)_2$ structure, the molecular weight of MAH–Pt–$(H_2O)_2$ is 457 $gmol^{-1}$. When $-CH_2$ bond is removed, the peak is observed at 415 *m*/*z*. If the 192 isotope is located, the molecular weight is 451 and 2 mol of H_2O is removed from the structure of MAH–Pt–$(H_2O)_2$ and the peak is observed at 443 *m*/*z*. This indicates that MAH–Pt has been synthesized.

Furthermore, Pt–N vibration bands at 552 and 441 cm^{-1} in FTIR spectrum show that Pt(II) was incorporated into MAH structure (Fig. 1b). Ligand exchange monomer, MAH–Pt(II)– cholic acid, was preorganized using MAH–Pt(II) and template, cholic acid. MAH–Pt(II) (0.1 mmol) and cholic acid (0.1 mmol) were dissolved in 5.0 mL of ethanol and the solution was stirred for 24 h.

2.3. Synthesis of gold–silver-nanoclusters and cholic acid imprinted gold–silver-nanoclusters sensor

The gold–silver-nanoclusters were prepared in a two-phase water/toluene system using a modified Brust method [29,30]. Briefly, nanoclusters were prepared by the dropwise addition of 0.01 M aqueous $NaBH_4$ solution in an equal volume of ammonical aqueous 0.5 mM $HAuCl_4$ (pH ca. 7.8) and 1 mM MAC in ethanol under vigorous stirring. 0.5 mM $AgNO_3$ was added to 40 mL of Au–MAC nanoclusters dispersion under continuous stirring. Au–Ag–MAC nanoclusters were separated and washed thoroughly several times with water and toluene and dried under nitrogen, followed by redispersion in dimethyl sulfoxide (DMSO). For the synthesis of Au–Ag nanoclusters having cholic acid imprinted nanoshell, methacryloyl-activated nanoclusters (having π bond for polymerization) were added into the reaction mixture containing the metal-chelate (MAH–Pt(II)–cholic acid) monomer (0.05 mmol) in DMSO, EDMA crosslinking monomer (0.4 mmol) and the initiator, AIBN (1 mol%) for the radical polymerization in ethanol. This solution was transferred into the dispersion medium and stirred magnetically at a constant stirring rate of 600 rpm in a glass polymerization tube. The polymerization tube was irradiated with UV light at 365 nm for 4 h. After the polymerization, cholic acid nanoshells having Au–Ag nanoclusters were separated from the polymerization medium. The residuals (e.g., unconverted monomer and initiator) were removed by a cleaning procedure. The resulting nanocrystals were treated with 12 mL (3/1, v/v) of 2 M NaOH/THF solution for 24 h to remove the templates (Fig. 2) [3]. Nonimprinted (NIP) Au–Ag nanoclusters sensor, without using cholic acid as template, was prepared in a similar way as described above and used as a reference.

2.4. Evaluation of nanocluster's luminesence

The sensing capability and specificity of the cholic acid memory having Au–Ag nanoclusters sensor was further explored by introducing cholic acid as a template molecule. Cholic acid adsorption studies were performed in a batch system. For this purpose, cholic acid was dissolved in ethanol and 20 mg of MIP clusters was placed in cholic acid solution at different concentrations (10^{-7} to 10^{-3} mol L^{-1}) for a period of 5 min at room temperature. The interactions between cholic acid and MIP particles were studied observing fluorescence measurements. The cholic acid imprinted Au–Ag nanoclusters showed a high separation between the excitation and emission wavelengths, simplifying fluorescence measurements, recorded photoluminescence spectra using spectrofluorometer. Cholic acid imprinted Au–Ag nanoclusters nanosensors were excited at 290 nm, and emission was recorded at 580 nm. Au–Ag nanoclusters having cholic acid imprinted nanoshell were tested against blood serum and urine.

3. Results and discussion

3.1. TEM characterization of nanoshell sensors

Fig. 3 shows TEM image of Au–Ag–MIP nanoclusters without cholic acid template after 2 M NaOH/THF acid (3/1, v/v) treatment. The shape of these nanoclusters is close to spherical and aggregated and with average size about 30 nm.

3.2. Raman characterization of nanoshell sensors

Au–MIP nanoparticles with cholic acid, and Au–MIP nanoparticles without cholic acid template were characterized with Raman spectroscopy (Fig. 4). In Raman spectrum of Au–MIP nanoparticles with cholic acid has band shifts at 1728 cm^{-1} because of cholic acid itself. These bands have been previously assigned [31]. The disappearance of that peak indicates the removal of template from the cholic acid imprinted nanoparticles.

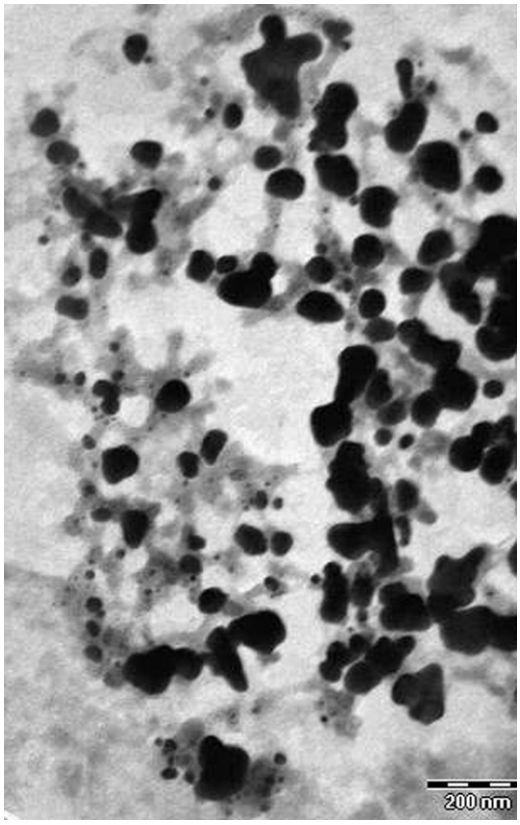

Fig. 3. TEM image of Au–Ag–MIP nanoclusters without cholic acid template (120 kV × 87,000).

3.3. Measurement of binding interactions of molecularly imprinted nanoshell sensor via photoluminescence

The functional metal-chelate monomer, [MAH–Pt(II)], was chosen to interact cholic acid, to form metal chelate and to make metal-complexing polymeric receptors for selective binding of cholic acid and analogues [25]. Metal chelate monomer and cholic acid molecule were mixed through preorganisation and this preorganisation complex defines the size and direction of the chemical interactions of the cholic acid imprinted cavity to prepare synthetic cholic acid receptor of Au–Ag nanoclusters (Fig. 2).

The selective binding ability and detection of cholic acid imprinted Au–Ag nanoclusters sensor were studied with fluorescence spectroscopy, and the results were given in Fig. 5. Cholic acid addition caused significant decreases in fluorescence intensity because they induced photoluminescence emission from Au–Ag nanoclusters through the specific binding to the recognition sites of the crosslinked nanoshell polymer matrix.

The analysis of the quenching results has been performed in terms of the Stern–Volmer equation. The mechanism of quenching of fluorescence has been explained by this way. A modified Stern–Volmer equation is derived to generate a linear calibration. Under optimum conditions, the fluorescence intensity versus cholic acid concentration gave a linear response according to Stern–Volmer equation with a 0.916 correlation coefficient (Fig. 6).

The fluorescence intensity of the cholic acid imprinted Au–Ag nanoclusters can be quenched by the addition of cholic acid. The quenching fluorescence intensity is proportional to cholic acid

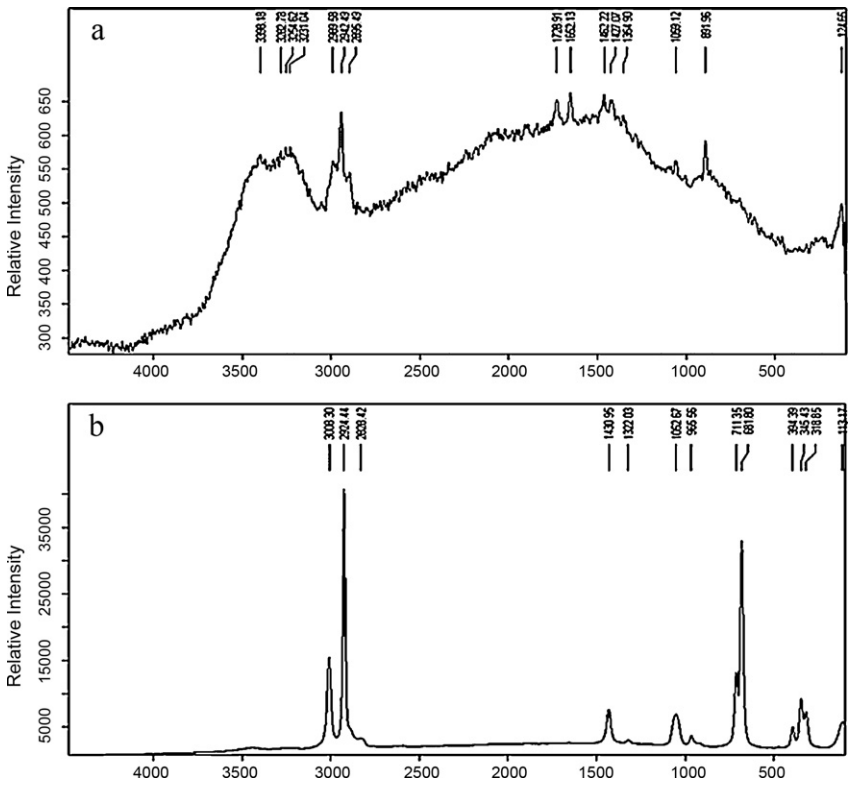

Fig. 4. Raman Images of (a) Au–Ag–MIP nanoclusters with cholic acid (unleached); (b) Au–Ag–MIP nanoclusters without cholic acid (leached).

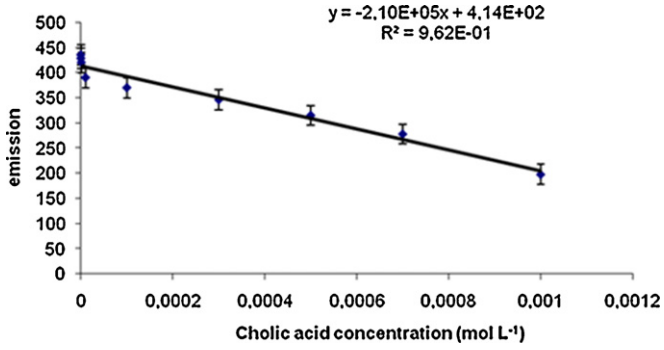

Fig. 5. The effect of concentration of cholic acid on the quenching of the fluorescence of the cholic acid imprinted Au–Ag nanoclusters (sensor specificity-adsorption isotherm).

concentration. The detection limit, defined as the concentration of analyte giving quenching of the fluorescence equivalent to three standard deviation of the blank plus the net blank quenching fluorescence, was 0.05 nmol mL^{-1}. The experiments were performed in replicates of three and the samples were analyzed in replicates of three as well. In the literature, the lowest detection limits have reported as 38.3 nmol mL^{-1} for deoxycholic acid (DCA) [32], 76.4 nmol mL^{-1} for ursodeoxycholic acid (UDCA) [33], 0.16 nmol mL^{-1} for bile acid [34], 5 nmol mL^{-1} for bile acid [35], 4.27 nmol mL^{-1} for cholic acid [36]. Although many methods have low detection limits, they are expensive [37–39]. So, this new cholic acid nanosensor is rapid and it has both low detection limit and very low cost.

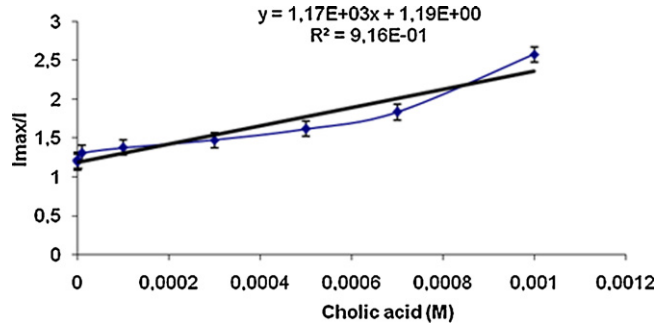

Fig. 6. Stern–Volmer-type description of the data.

Au–Ag nanoclusters having cholic acid imprinted nanoshell were tested against blood serum and urine. Three different blood serum and urine samples which belong to healthy persons were also examined with Au–Ag nanoclusters and average cholic acid level was found to be 6 and 2.5 respectively. The amount of colic acid in the blood of a healty person is about 6 μM [40]. Therefore, the results obtained showed that these nanoclusters can be used for the determination.

The affinity constants of cholic acid can be estimated from the thermodynamic analysis of the fluorescence intensity as a function of the cholic acid concentration based on Scatchard analysis [41,42] and Langmuir isotherm [43].

If we consider a binding equilibrium such as:

$$\text{Cholic acid} + (\text{Au–Ag})_{\text{nanocluster}} \overset{k}{\rightleftharpoons} \text{cholic acid} - (\text{Au–Ag})_{\text{nanocluster}} \quad (1)$$

where, cholic acid and $(\text{Au–Ag})_{\text{nanocluster}}$ represent cholic acid in the solution and cholic acid imprinted polymeric nanoshell having nanocluster, respectively, and cholic acid $(\text{Au–Ag})_{\text{nanocluster}}$ is the cholic acid–nanocrystal bound complex. A Scatchard relationship can be obtained using the following equation.

$$\frac{I}{C_o} = \frac{I_{max}}{K_D} - \left(\frac{I}{K_D}\right) \quad (2)$$

where, K_D is the equlibrium dissociation and I is the fluorescence intensity. A plot of I versus I/C gave a straight line and the equlibrium binding constants ($K_a = 1/K_D$) were given in Table 1.

Table 1
Comparison of Langmuir and Scatchard analysis for cholic acid imprinted nanoparticle.

Rebound molecules	Langmuir K_a (M^{-1})	I_{max} (a.u.)	Scatchard, K_a (M^{-1})	I_{max} (a.u.)
Cholic acid	2.73×10^4	221	2.13×10^8	283

Table 2
Selectivity of cholic acid imprinted Au–Ag nanosensor.

	C (mol L^{-1})	Emission (MIP)	MIP (mol L^{-1})	NIP (mol L^{-1})	k MIP	k NIP	k'
Cholic acid	1×10^{-4}	370	1×10^{-4}	1.26×10^{-6}			
Chenodeoxycholic acid	1×10^{-4}	414	1.23×10^{-6}	2.3×10^{-7}	81	5.5	14.7

The validity of the Langmuir isotherm can be tested by determining the affinity constant measuring the fluorescence intensities at equlibrium with different bulk concentrations (5×10^{-8} to 10^{-3} mol L^{-1}) (Fig. 5). Langmuir relationship can be obtained using the following equation;

$$\frac{C_o}{I} = \frac{1}{I_{max} \cdot b} + \frac{C_o}{I_{max}} \quad (3)$$

The results obtained from the linearized form of the Langmuir isotherm, by plotting C_o/I as a function of C_o, and the Scatchard analysis findings are also given in Table 1. Association constant, K_a, and the apperant maximum number of recognition sites, I_{max}, values for the specific interaction between the template imprinted polymer of the nanoparticles and the template itself were compared in Table 1. As seen from Table 1, in general, the magnitude of K_a (2.73×10^4 mol L^{-1}, 2.13×10^8 mol L^{-1}, based on Langmuir and Scatchard analysis, respectively) is due to the accessibility of cholic acid template molecules. Some template cavities formed during imprinting process were stayed inside the polymer matrix of the nanoclusters.

The K_a and I_{max} values estimated from Scatchard analysis are very close to the Langmuir analysis data and cholic acid templated sites of nanocrystals are highly selective to the cholic acid recognition sites. So, the based on Scatchard analysis for the binding of cholic acid to MIP nanosensor, K_a and I_{max} were found to be 2.13×10^8 M^{-1} and 283, respectively. The value of K_a suggests that affinity of the binding sites is very strong.

3.4. Recognition selectivity of cholic acid imprinted nanoshell sensor

Molecular imprinting process with cholic acid gives a cavity that is selective for cholic acid and its analogues. Cholic acid imprinted nanocrystals were treated with chenodeoxycholic acid which has very similar molecular structure with cholic acid in order to check whether the nanoshell has any effect on recognition process. The obtained results indicated that MIP nanosensor has 92 times greater selectivity for cholic acid than that of chenodeoxycholic acid. The investigation of fluorescence intensity of NIP did not show a significant change in fluorescence intensity. The selectivity coefficient, k, of cholic acid and chenodeoxycholic acid was found to be 81 for MIP particles and 5.5 for NIP particles and relative selectivity coefficient, k', was determined as 14.7. As seen that, MIP sensor is 14.7 times selective with respect to NIP sensor (Table 2). Obtained results clearly indicated that the change of fluorescence intensity is due to specific binding between cholic acid and cholic acid memory sites having nanoparticles.

The cholic acid can simultaneously chelate to Pt(II) metal ion and fit into the shape-selective cavity. So, this interaction between Pt(II) ion and free coordination spheres has an effect on the binding ability of the Au–Ag nanoclusters. Experimental results showed that shape-selective cavity formation was occured for cholic acid.

4. Conclusion

We have developed a novel chemical preparation method for methacryloyl based self-assembled monolayer and to make up imprinting polymer via ligand exchange of cholic acid on Au–Ag nanoclusters. The cholic acid imprinted MAH–Pt(II)–cholic acid copolymer of Au–Ag nanoshell is expected to bind cholic acid. The results showed that the change in fluorescence could be attributed to the high complexation geometric shape affinity (or cholic acid memory) between cholic acid molecules and cholic acid cavities occured on the Au–Ag nanoshells. In conclusion, the cholic acid imprinted nanoshell sensor has been gaining widespread recognition as a sensor for cholic acid because the imprinting methods create a nanoenvironment based on shape of cavity memorial, size and positions of functional groups that recognizes the imprinted molecule, cholic acid, based on ligand-exchange imprinting methods. Nanoshell sensor having cholic acid templates responses to cholic acid and its analogues through fluorescence intensity decrease. The fluorescence intensity correlates to the amount of cholic acid analogues bounded to the nanoshell having Au–Ag nanoclusters in the cases of incubating the cholic acid imprinted nanoclusters sensor with the cholic acid aqueous solution. The fluorescence intensity decreased with increase concentration of cholic acid.

References

[1] W.H. Mandeville, D.I Goldberg, Curr. Pharm. Des. 3 (1997) 15–28.
[2] W.H. Mandeville, W. Braulin, P. Dhal, A. Guo, C. Huval, K. Miller, Mater. Res. Soc. Symp. Proc. 550 (1999) 3–15.
[3] Y. Wang, J. Zhang, X.X. Zhu, A. Yu, Polymer 48 (2007) 5565–5571.
[4] B.L. Lee, A.L. New, C.N. Ong, J. Chromatogr. B 704 (1997) 35–42.
[5] J.M. You, Y.W. Shi, Y.F. Ming, Z.Y. Yu, Y.J. Yi, J.Y. Liu, Chromatographia 60 (2004) 527–535.
[6] M. Nobilis, M. Pour, J. Kunes, J. Kopecky, J. Kvetina, Z. Svoboda, K. Sladkova, J. Vortel, J. Pharm. Biomed. Anal. 24 (2001) 937–946.
[7] A. Criado, S. Cardenas, M. Gallego, M. Valcarcel, J. Chromatogr. B 792 (2003) 299–305.
[8] A. Roda, C. Cerre, P. Simoni, C. Polimeni, C. Vaccari, A. Pistillo, J. Lipid Res. 33 (1992) 1393–1402.
[9] K. Bentayeb, R. Batlle, C. Sánchez, C. Nerín, C. Domeno, J. Chromatogr. B 869 (2008) 1–8.
[10] O. Ramstrom, K. Mosbach, Curr. Opin. Chem. Biol. 3 (1999) 759–764.
[11] S. Striegler, J. Chromatogr. B: Biomed. Sci. Appl. 804 (2004) 183–195.
[12] M. Odabaşi, R. Say, A. Denizli, Mater. Sci. Eng. C 27 (2007) 90–99.
[13] H. Yavuz, R. Say, A. Denizli, Mater. Sci. Eng. C 25 (2005) 521–528.
[14] B.D Fahlman, Materials Chemistry, vol. 1, Springer, Mount Pleasant, MI, 2007, pp. 282–283.
[15] J.P. Borra, J. Phys. D: Appl. Phys. 39 (2006) R19–R54.
[16] F.E. Kruis, H. Fissan, A. Peled, J. Aerosol Sci. 29 (1998) 511–535.
[17] N.S. Tabrizi, M. Ullmann, V.A. Vons, U. Lafont, A. Schmidt-Ott, J. Nanopart. Res. 11 (2009) 315–332.
[18] V. Abdelsayed, K.M. Saoud, M.S. El-Shall, J. Nanopart. Res. 8 (2006) 519–531.
[19] L.M. Liz-Marzan, P.V. Kamat, Nanoscale Mater. (2003).
[20] A.S. Edelstein, R.C. Cammarata (Eds.), Institute of Physics, 1996, pp. 347–373.
[21] G. Guan, B. Liu, Z. Wang, Z. Zhang, Sensors 8 (2008) 8291–8320.
[22] A. Gültekin, S.E. Diltemiz, A. Ersöz, N.Y. Sarıözlü, A. Denizli, R. Say, Talanta 78 (2009) 1332–1338.
[23] A.B. Kharitonov, A.N. Shipway, I. Willner, Anal. Chem. 71 (1999) 5441–5443.
[24] J. Matsui, K. Akamatsu, S. Nishiguchi, D. Miyoshi, H. Nawafune, K. Tamaki, N. Sugimato, Anal. Chem. 76 (2004) 1310–1315.

[25] I. Lampronti, N. Bianchi, C. Zuccato, A. Medici, P. Bergamini, R. Gambari, Bioorg. Med. Chem. 14 (2006) 5204–5210.
[26] S.E. Diltemiz, R. Say, S. Büyüktiryaki, D. Hür, A. Denizli, A. Ersöz, Talanta 75 (2008) 890–896.
[27] R. Say, B. Garipcan, S. Emir, S. Patır, A. Denizli, Colloids Surf. A: Physicochem. Eng. Aspects 196 (2002) 199–207.
[28] S.E. Diltemiz, A. Denizli, A. Ersöz, R. Say, Sensors Actuat. B 133 (2008) 484–488.
[29] M. Brust, D. Bethell, C.J. Kiely, D.J. Schiffen, Langmuir 14 (1998) 5425–5429.
[30] J. Sharma, N.K. Chaki, A.B. Mandele, R. Pasricha, K. Vijayamohanan, J. Colloid Interface Sci. 272 (2004) 145–152.
[31] E. Lamcharfi, C.C. Solal, M. Parquet, C. Lutton, J. Dupre, C. Meyer, Eur. Biophys. J. 25 (1997) 285–291.
[32] V.G. Rodriguez, E. Silvia, G.C. Lucangioli, F. Otero, C.N. Carducci, J. Pharm. Biomed. Anal. 23 (2000) 375.
[33] M.G. Quaglia, A. Farina, E. Bossù, C. D'Aquila, A. Doldo, J. Pharm. Biomed. Anal. 16 (1997) 281.
[34] Y.S. Li, W.P. Liu, X.F. Gao, D.D. Chen, W.G. Li, Biosen. Bioelectron. 24 (2008) 538–544.
[35] L. Ye, S. Liu, M. Wang, Y. Shao, M. Ding, J. Chromatogr. B 860 (2007) 10–17.
[36] X. Rana, Q. Liang, G. Luoa, Q. Liu, Y. Pan, B. Wang, C. Pang, J. Chromatogr. B 842 (2006) 22–27.
[37] M. Scherer, C. Gnewuch, G. Schmitz, G. Liebisch, J. Chromatogr. B 877 (2009) 3920–3925.
[38] S.J.J. Tsai, Y.S. Zhong, J.F. Weng, H.H. Huang, P.Y. Hsieh, J. Chromatogr. A 1218 (2011) 524.
[39] X. Xiang, Y. Han, M. Neuvonen, J. Laitila, P.J. Neuvonen, M. Niemi, J. Chromatogr. B 878 (2010) 51–60.
[40] T. Murai, R. Mahara, T. Kurosawa, A. Kimurab, M. Tohmaa, J. Chromatogr. B 691 (1997) 13–22.
[41] P.Y. Tsoi, J. Yang, Y.T. Sun, S.F. Sui, M.S. Yang, Langmuir 16 (2000) 6590–6596.
[42] M. Yang, P.Y. Tsoi, C.W. Li, J. Zhao, Sensors Actuat. B 115 (2006) 428–433.
[43] B. Persson, K. Stenhag, P. Nilsson, A. Larsson, M. Uhlen, P.A. Nygren, Anal. Biochem. 246 (1997) 34–44.